EPA/600/A-93/292

PHYSICAL MODELING OF THE FLOW FIELD AROUND TWIN HIGH-RISE BUILDINGS

Robert E. Lawson, Jr.
Atmospheric Sciences Modeling Division
Air Resources Laboratory
National Oceanic and Atmospheric Administration
Research Triangle Park, NC 27711

and

Masaaki Ohba
Tokyo Institute of Polytechnics
Atsugi, Kanagawa Pref., Japan 243-02

1. INTRODUCTION

In Japan, many high-rise office buildings have been built in downtown areas in order to more effectively use the available space in commercial districts. These buildings are often designed to have two high-rise structures atop a common, terrace-shaped lower level. This configuration serves to protect pedestrians on the sidewalk from the strong winds which occur due to blockage of the approach flow by the high-rise buildings.

Typically, as many as 5000 people might work in these buildings each day. As a result, the heat gain/loss inside these buildings is so great that electrical generating plants are necessary in order to provide building air conditioning for maintaining a comfortable working environment. If these generating plants were installed near the high-rise buildings, they would generally be installed in an underground level and any exhaust would be emitted into the area near the base of the high-rise buildings. Because of their energy efficiency, co-generation systems are widely used for producing heat and electricity, but these co-generation systems emit large amounts of NO_x so that they may contribute significantly to increases in air pollution around the buildings. Hence, installation of such co-generation systems near the base of the high-rise buildings may result in adverse effects on human health.

Many researchers have investigated air pollution problems around buildings, but these experiments have concentrated primarily on examination of the flow structure and dispersion in the vicinity of an isolated building. Since high-rise buildings are typically located in a complex city environment, and since the twin high-rise structure introduces the additional complexity of a nearby building, the available data is of limited use in evaluating contaminant levels.

In this wind tunnel experiment, we selected three basic types of high-rise buildings and investigated the effects of these buildings on both gaseous diffusion and flow structure. This report describes the flow-field measurements, the techniques used to measure the flow field and some conclusions which can be drawn from the measurements. A companion paper (Ohba and Lawson, 1993) describes the concentration measurements. The primary purposes of this portion of the study were :

- to examine the centerline mean streamline patterns and, hence, determine which possible source locations would be likely to cause adverse concentrations on the building surface
- to determine whether the addition of a terrace level significantly altered the flow field
- to determine how the flow field in the downstream wake of the downwind building changed as a result of varying the building height and the separation between the buildings
- to obtain flow-field data for comparison with the results of numerical simulations based on a k-ε model.

2. SIMILARITY CRITERIA

Similarity criteria for modeling flow around a building immersed in a neutral atmospheric boundary layer in a wind tunnel require that the Rossby number, Reynolds number, Peclet number or Reynolds-Schmidt product, plus a set of non-dimensional boundary conditions be matched in both model and prototype. Referring to Snyder (1981), the Rossby number can be neglected when modeling prototype flows with a length scale less than about 5 km. Also, provided the model Reynolds number is sufficiently large, it is not necessary to match the Reynolds number, Peclet number or Reynolds-Schmidt product between model and prototype. The reference velocity in this study was chosen such that the building Reynolds number was greater than

*On assignment to the Atmospheric Research and Exposure Assessment Laboratory, U.S. Environmental Protection Agency.

that regarded as the critical value for Reynolds number independence (Golden, 1961). The Reynolds number based on the wind speed at the top of the smallest building was approximately 33,000.

For geometrical similarity, the details of the prototype of size smaller than the roughness length need not be reproduced in the model. All of the models used in this study had smooth walls and sharp edges with no artificial roughening of the building surfaces.

The general setting was assumed to be an environment typical of the downtown areas of modern cities. Ideally, the building height, shape and separation between the buildings should all be varied over the full range of typical values; however, the total number of combinations would quickly become excessive. We therefore restricted the number of parameters to four building heights, five building shapes and several separation distances between the twin building models. Only one parameter was varied at a time while maintaining all other parameters at their base-case values.

3. WIND TUNNEL

The experiments were carried out in the wind tunnel of the U.S. Environmental Protection Agency's Fluid Modeling Facility (Snyder, 1979). The wind-tunnel is of the open-return type with a test section 3.7 m wide, 2.1 m high and 18.3 m long. The air speed through the test section can be varied from about 1 to 10 m/s. An automated instrument carriage system is located inside the tunnel test section and is driven by a microcomputer linked to the data acquisition system. It provides the capability for positioning a probe anywhere in the test section, acquiring data, then moving to the next measurement location and repeating the process, entirely without intervention. This automated instrument carriage system enabled the (normally tedious) process of making pulsed-wire measurements to be carried out around-the-clock.

A simulated neutral atmospheric boundary layer was created in the wind tunnel using spires and floor roughness elements. The spires were patterned after those designed by Irwin (1981). In this study, the spires were chosen to produce a boundary layer with depth of 2000mm and a power law exponent of about 0.3. Block roughness elements were used downstream of the spires to maintain the boundary layer in equilibrium.

4. BUILDING MODELS

The high-rise building models used in this study were rectangular blocks with heights (H_b) of 300, 450, 600 and 1200mm, respectively, with building width and length fixed at 200mm. These correspond to full-scale dimensions of 75, 112.5, 150 and 300m, respectively, in accordance with the scale ratio of 250:1. The terrace-shaped building model was 150mm high, 1000mm wide and 1400mm long, corresponding to full-scale dimensions of 37.5m x 250m x 350m. The building models were centered on a point 11.37m downwind of the leading edge of the spires.

5. ANEMOMETRY

5.1 *Pulsed-Wire Anemometer*

The bulk of the measurements were made with a pulsed wire anemometer (PWA). The principle of operation of the PWA is straightforward. The probe consists of three fine wires, two outside wires being parallel to one another and a central wire being perpendicular to the outer ones. The central wire is pulsed with a high current for a few microseconds which raises the temperature of the wire to several hundred degrees Celsius. This releases a tracer of heated air into the flow and it is convected away with the instantaneous velocity of the air stream. The two outside wires are operated as resistance thermometers and are used to measure the time-of-arrival of the heated air parcel. The use of two sensor wires, one on either side of the pulsed wire, ensures that the flow direction is unambiguously determined .

The PWA probe can be oriented to measure velocity components in all three coordinate directions. Because of finite wire lengths, the probe has a yaw response up to about to 70°, so that, for reasonable measurements of traverse components of the flow, the turbulence intensity must be relatively high, e.g., above 20 to 25%. For low-intensity flows, the hot-wire anemometer may be preferable.

PWA calibrations were performed against a Pitot-static tube mounted in the free-stream of the wind tunnel with the spires laid down on the wind tunnel floor. A capacitance manometer was used with the Pitot tube to determine reference velocities in the range of 0.5 to 5m/s. An iterative least-squares procedure was used to obtain a "best-fit" of these calibration points to the equation

$$U = A/T + B/T^2 + C/T^3,$$

where U is the wind speed indicated by the Pitot-static tube, T is the time-of-flight, and A, B and C are constants. A typical calibration curve is shown in Figure 1.

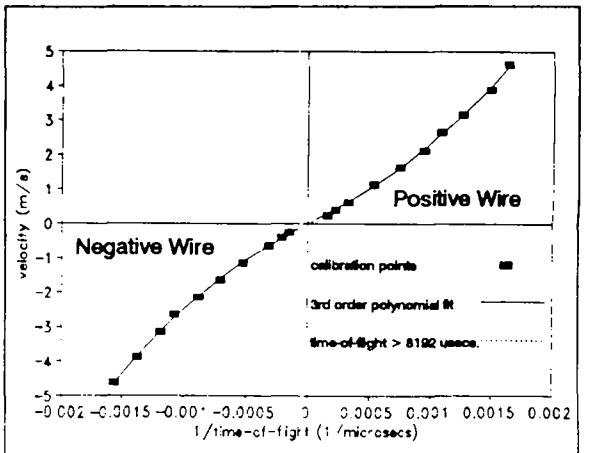

Figure 1. Typical PWA calibration curves.

All of the PWA measurements described in this report were obtained using a pulsing rate of 10Hz and an averaging time of 120 seconds. The data acquisition computer converted the 12-bit digital time-of-flight signal from the PWA to velocity using the appropriate calibration curve for each sensor, computed statistics, then displayed and plotted the results in real time.

5.2 *Hot-Wire Anemometer*

X-array sensors were used with a hot-wire anemometer (HWA) to measure the mean velocity and turbulence intensity profiles of the approach flow in the absence of any buildings. Calibrations were performed over a range of 0.5 to 5 m/s in the same manner as the pulsed wire anemometer. The calibration voltages were used to calculate a set of best-fit parameters to a King's law form of equation

$$E^2 = A + BU^n,$$

where E is the anemometer output voltage, U is the mean wind speed, and A,B and n are constants that are determined by a least-squares fitting procedure. The HWA is useful when the turbulence intensities are relatively low (e.g. 20% or so), or where the instantaneous velocity vector remains within a cone with a total angle of about 30°. Significant errors can occur when the hot-wire anemometer is used in high-intensity or reversing flows such as that found near buildings or obstacles.

The analog output signals from the HWA were digitized at a rate of 1000Hz and linearized and processed on a microcomputer using a 12-bit analog-to-digital converter. A 60-second averaging time was used for all mean measurements. All time-series measurements were obtained over a period of 300s at a sample rate of 2000Hz.

6. EXPERIMENTAL CONDITIONS

Table 1 contains pertinent experimental parameters used in this study. Figure 2 shows the reference geometry. The reference velocity was maintained at 3.5 m/s at a position of X=0mm and Z = 600mm during all measurements.

Table 1. Experimental parameters.

Case No.	Ht. (m) Hb	Sep. L/Hb	Case No.	Ht. (m) Hb	Sep. L/Hb
1	0.60	0.00	9	0.30	0.75
2	0.60	0.50	10	0.30	1.00
3	0.60	0.50	11	0.60	0.25
4	0.60	0.25	12	0.60	0.75
5	0.60	0.75	13	0.60	1.00
6	0.60	1.00	14	1.20	0.25
7	0.30	0.25	15	1.20	0.50
8	0.30	0.50	16	1.20	0.75

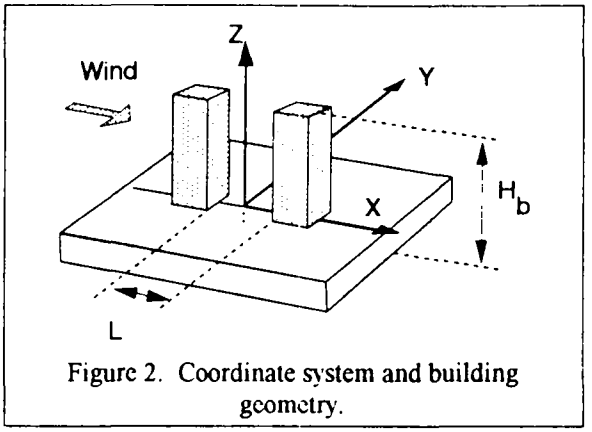

Figure 2. Coordinate system and building geometry.

Vertical and lateral velocity profiles were first obtained in the absence of any buildings in order to characterize the simulated boundary layer. For Cases 1 through 3, longitudinal and vertical components of velocity were measured in the vertical centerplane. Longitudinal and lateral components were measured in a single horizontal plane 50mm above the surface.

In Cases 4 through 6, only the longitudinal and vertical components were measured on the vertical centerplane downstream of the downwind building. For Cases 7 through 16, only the longitudinal component was measured downwind of the downstream building. The high-rise building models were situated atop a terrace section only for Cases 3 through 6.

7. RESULTS AND DISCUSSION

7.1 *Boundary Layer Characterization*

Figures 3 and 4 show profiles of the longitudinal mean velocity and all three components of turbulence

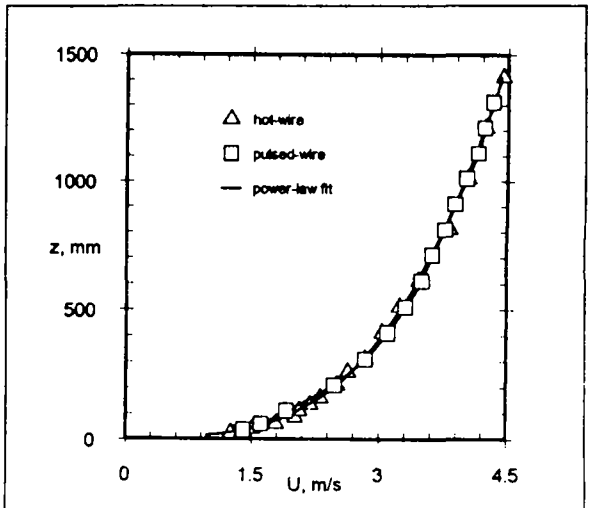

Figure 3. Approach flow velocity profiles.

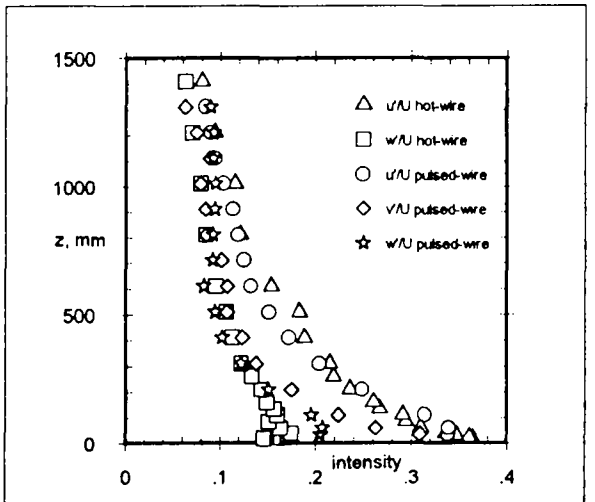

Figure 4. Approach flow turbulence intensity.

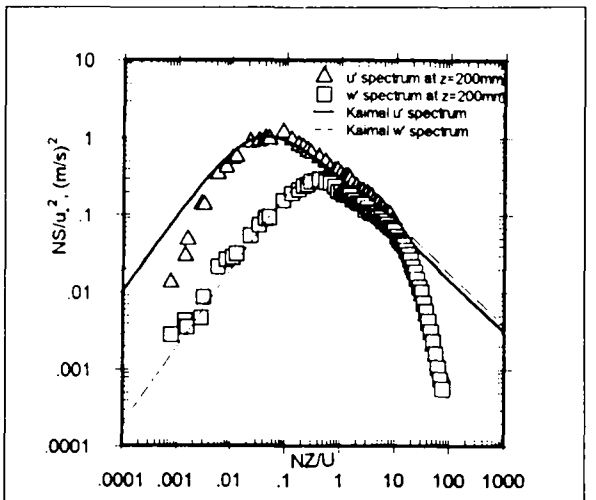

Figure 5. Approach flow turbulence spectra.

intensity measured near the center of the test area. Measurements with the HWA were at X = 0mm while measurements with the PWA were slightly further upwind at X=-700mm. The mean velocity profile was found to fit well to the power law $U(Z) = 0.522(Z+10)^{0.295}$. A log-law fit to the mean velocity profile over the range $0< Z < 200$mm yielded a roughness length of 5.9mm (~1.5m full-scale), a displacement height of 28mm and a friction velocity of 0.273 m/s. These values are consistent with those obtained by Cook (1973) and the power law exponent falls within the range of full-scale values from ESDU(1972). The vertical component of turbulence intensity measured at the upstream location is slightly greater than that at X=0 due primarily to proximity to individual roughness elements.

Lateral profiles of mean velocity and turbulence intensity were measured at heights of 200, 500 and 1000mm near the center of the test area. These lateral profiles indicated peak deviations over the width of the test section on the order of ± 0.1 m/s (apparently an artifact of the spires), but deviations were deemed acceptably small near the center of the test area.

Time-series of digitized velocities were collected at heights of 200, 500 and 1000mm, and were subsequently analyzed to obtain turbulence spectra. Figure 5 shows both the u' and w' spectra. The solid and dashed lines represent the surface layer spectra due to Kaimal *et al* (1972). In accordance with the model scale ratio of 250:1, the measuring height of Z = 200mm corresponds to a full-scale height of 50m. The wind tunnel spectra at this level compare favorably with the Kaimal spectra, hence the boundary layer simulates the prototype atmospheric boundary layer reasonably well.

7.2 *Mean Velocity Vectors and Streamlines*

Figures 6a through 8b show the mean velocity vectors around the building models as measured with the pulsed wire anemometer and streamlines constructed from these measurements.

In the U-W flow field for Case 1 (Figure 6a), a stagnation point was observed on the upwind face of the building model near $Z/H_b \cong 2/3$. Below this level, the oncoming flow flowed downward along the upwind face and reached ground level. The flow separated on the upwind edge of the rooftop and reattached on the rooftop. Reverse flow was not clearly seen on the rooftop because there were no data points sufficiently close to the surface. A recirculating eddy was formed just downstream of and slightly below the top of the building. Centerplane mean streamlines constructed from the measurements clearly show the salient features of the flow. The streamline pattern is topologically consistent with the results of Davies *et al* (1980) for a square-section building with height six times its width; however, the center of the recirculating eddy is located below the top of the building in the present case. The taller building used by Davies *et al* showed fully separated flow on top of the building and this is probably a controlling factor in determining the height of the downwind eddy. An elevated "free stagnation point" was observed downstream near $Z/H_b \cong 1/2$. In the U-V flow field at Z = 50 mm (Figure 6b), the flow separated at the upwind edge of the building model and reattached on the side. Streamlines constructed from measurements in the horizontal plane assume that vertical motion near the surface is restricted sufficiently to allow two-dimensional streamlines to be representative of the near-surface flow. It is clear from the streamline patterns that emissions from sources located near the surface in the downwind wake of the building will be swept directly toward the downwind face of the building.

The U-W flow field for Case 2, like that for Case 1, shows the flow separating on the upwind rooftop edge of the upwind building model and reattaching on the same rooftop (see Figure 7a). After reattachment, the flow was directed downwards along the upwind face of the downwind building model and was directed upstream at the position of $Z/H_b \cong 1/3$. A recirculating flow was clearly created between the twin building models. In the areas near the rooftop of the downwind building model, the flow was parallel to the

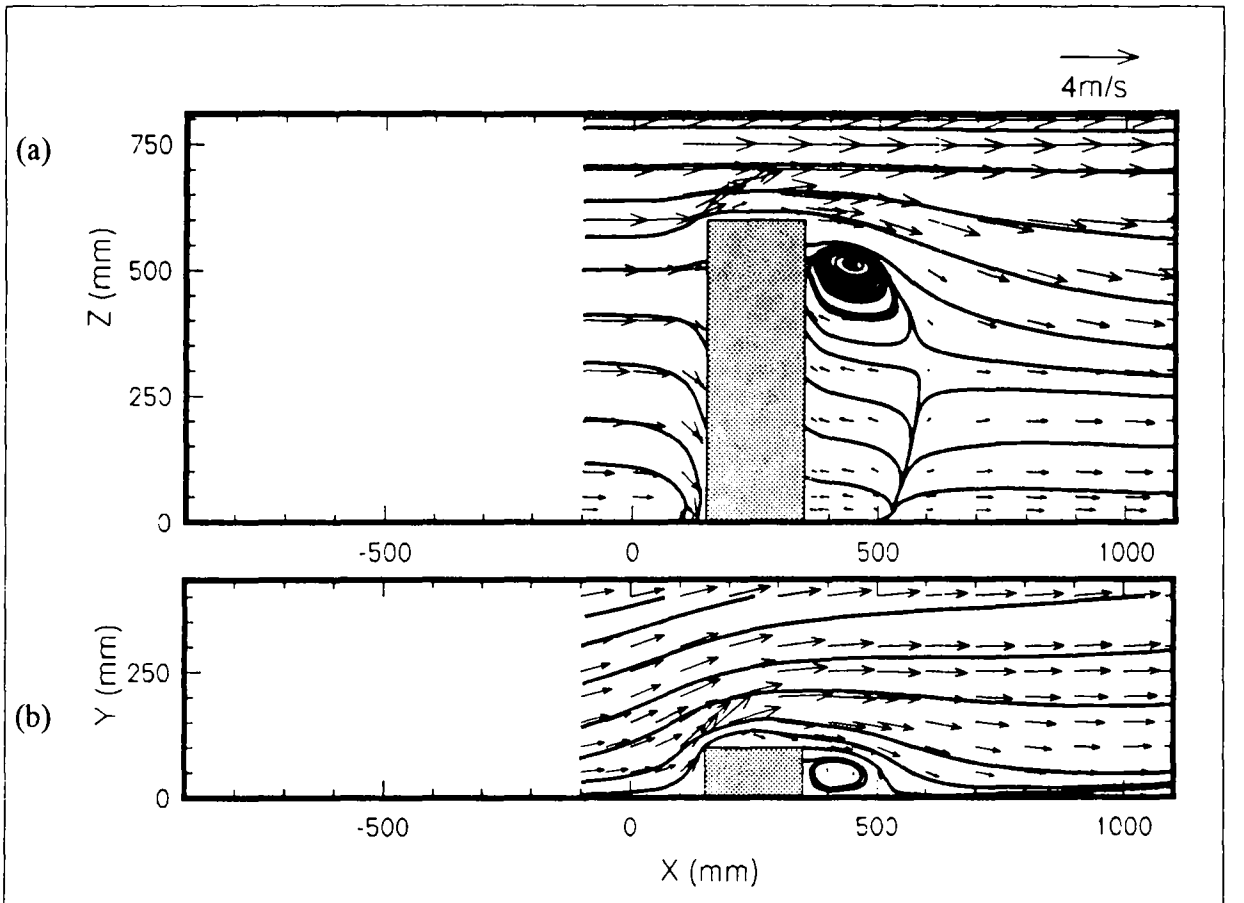

Figure 6. Velocity vectors and streamlines for Case1 in the (a) vertical centerplane and (b) in a horizontal centerplane at an elevation of 50mm.

rooftop line, indicating that separated flow did not occur on the upwind edge of the rooftop. This suggests that the upwind building model produced high turbulence downstream of the model and that the turbulence acted to retard separation on the downwind building model. The reverse flow region in the near-wake behind the downwind model was not as clearly defined as that between the twin buildings. The streamlines downstream of the downwind building again appear to be topologically consistent with the results of Davies *et al*, but the "free stagnation point" is located nearer the surface. The velocity vectors in the U-V plane (Figure 7b) similarly show separation being retarded on the sides of the downwind building. The streamlines in the U-W plane show recirculating flow between the twin building models and behind the downwind building model, respectively. Again, emissions released near the surface in the near wake of the downwind building will be swept directly toward the downwind face of the downwind building.

For Case 3, a terrace-type basement was added to the buildings for Case 2 while maintaining the building height constant. The reverse flow region between the twin buildings was more clearly defined in the U-W flow field (Figure 8a) than for Case 2. A large, persistent eddy filled the region between the buildings. Small regions of reverse flow appeared upstream and downstream of the terrace section. Separation on the roof of the downwind building was again retarded. The recirculation zone in the wake of the downwind building hardly differed from the previous cases, but the elevated stagnation point occurred much nearer to the surface. In Figure 8b, the U-V flow field showed little difference from that observed for Case 2. As in the previous cases, emissions from sources located in the near-wake of the downwind building will be swept directly to the downwind face of the downwind building.

In Cases 4 through 6, the separation distance between the twin building models was varied while maintaining all other parameters the same as in Case 3. When L/H_b was equal to 1.0, separated flow was again observed on the rooftop of the downwind building model. Hence the effect of the upwind building on flow around the downwind building appears to be greatly diminished for $L/H_b \geq 1.0$. Curiously enough, this separation criterion appears to coincide with the observations of Wise (1971, as summarized by Britter and Hunt, 1979) regarding conditions

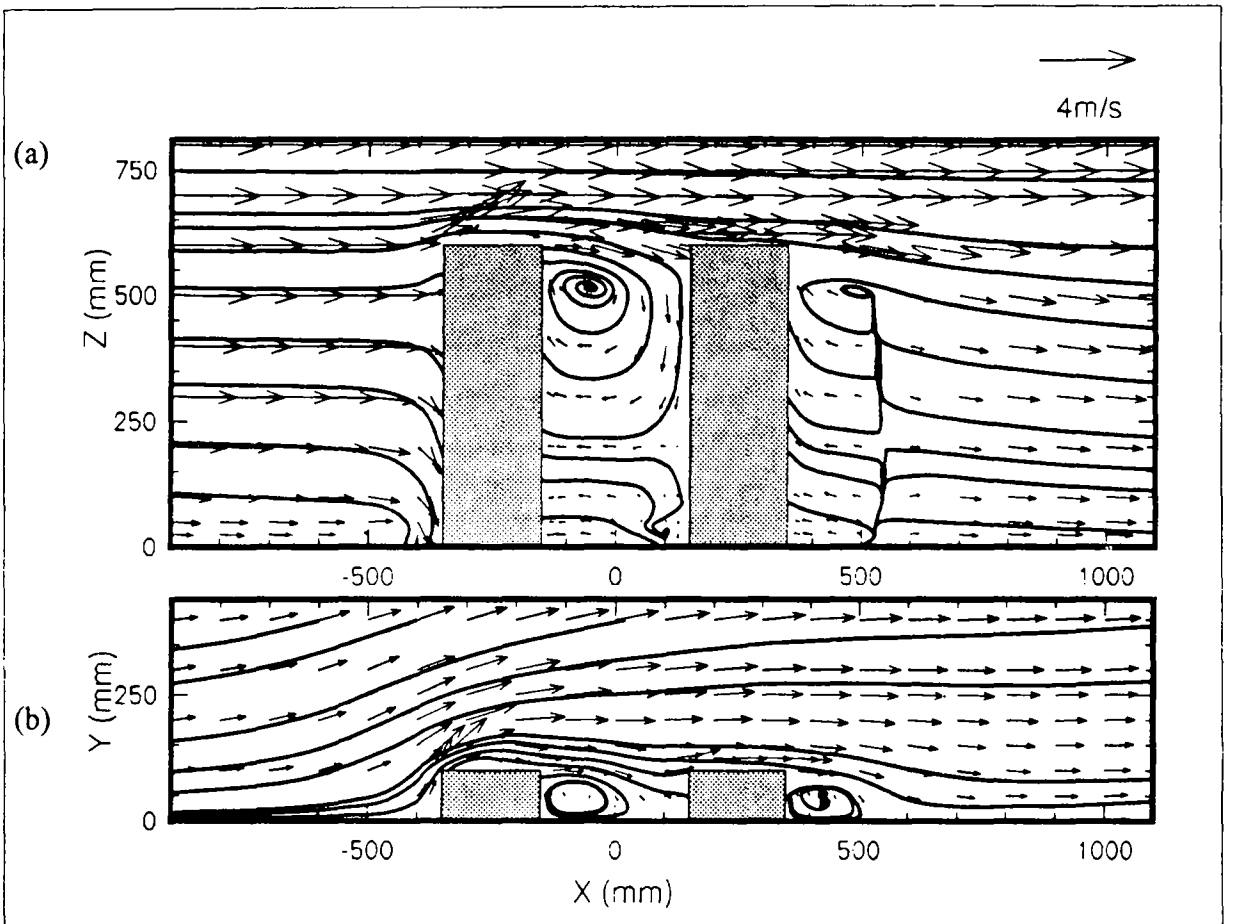

Figure 7. Velocity vectors and streamlines for Case2 in the (a) vertical centerplane and (b) in a horizontal centerplane at an elevation of 50mm .

under which the wind speed near the ground between the two buildings would reach a maximum.

7.3 *Reattachment Length Behind The Downwind Building*

The longitudinal distance from the downwind face of the downwind building to the point of reattachment of the flow to the ground surface behind the downwind building was measured using the pulsed wire anemometer. Figure 9 shows the definition of the reattachment length behind the downwind building model. Note that the term reattachment is used in a very broad sense in this context. The flow downstream of the buildings is highly complex and three-dimensional; the term reattachment, as seen in the diagram, really describes the location near the surface or terrace level where the sign of the longitudinal velocity component changes from negative (upstream) to positive (downstream). Figure 10 presents the relationship between reattachment lengths and separation distances of the twin building models. From Figure 10, it was found that the normalized reattachment length increased as the building height increased, but the separation distances of the twin building models did not greatly influence the reattachment length for separation distances in the range of $0.25 \leq L/H_b \leq 1.0$.

8. SUMMARY AND CONCLUSIONS

Velocity vectors around high-rise building models immersed in a simulated atmospheric boundary layer were measured with a pulsed wire anemometer. Streamlines were constructed from these data to illuminate the basic flow features and to show where exhaust emissions near the base of the downwind building might impact the building. Measurements were accomplished with a single building, two buildings with various heights and separations, and with the addition of a terrace level. A recirculating eddy was observed in the mean flow field just downstream and near the top of the high-rise building models. From these wind tunnel experiments, the following conclusions are drawn:

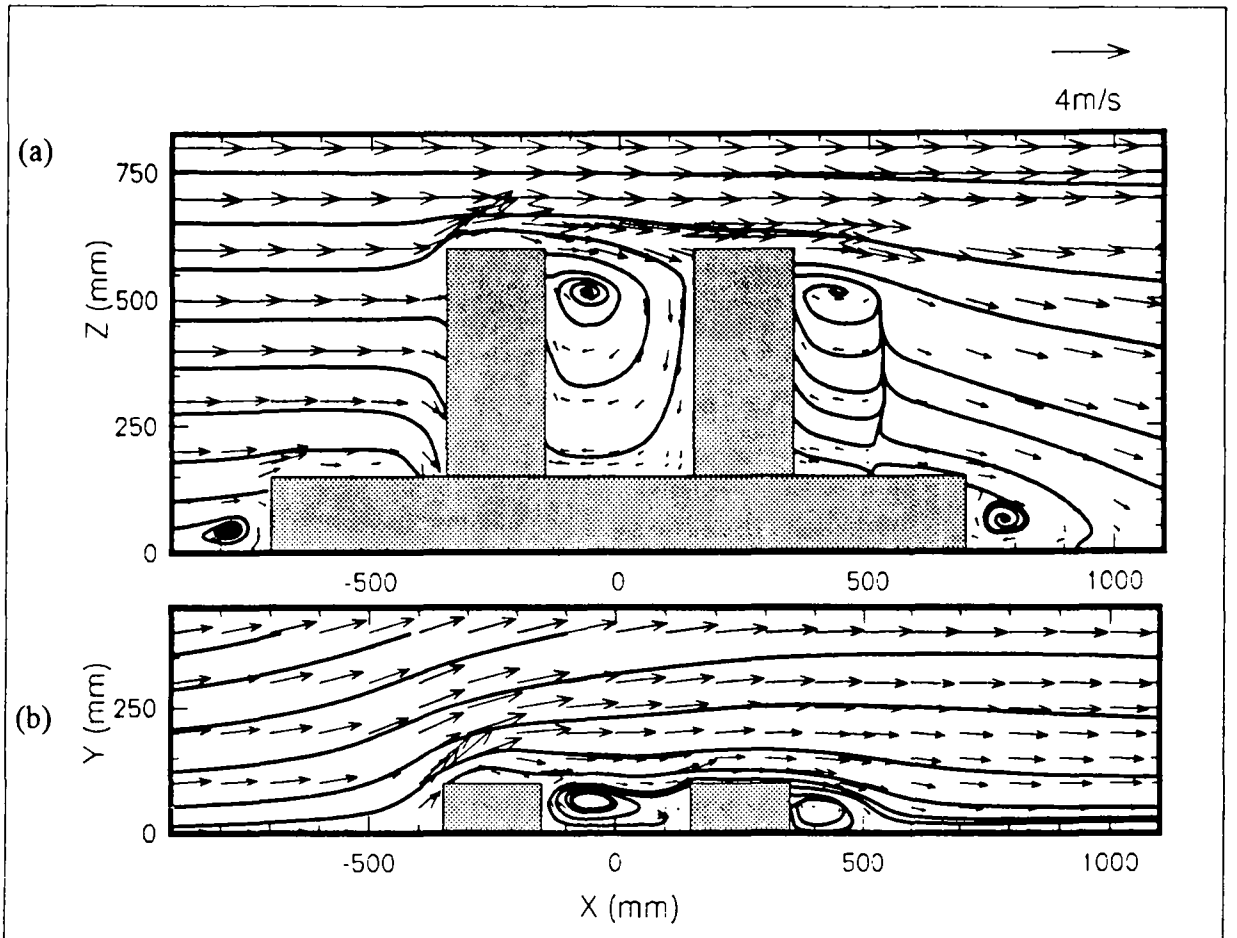

Figure 8. Velocity vectors and streamlines for Case3 in the (a) vertical centerplane and (b) in a horizontal centerplane at an elevation of 50mm.

(1) The primary effect of the upwind building is to retard flow separation on the top and sides of the downwind building.

(2) The effects of the upwind building on flow separation near the top of the downwind building are diminished when the separation (L/H_b) equals or exceeds 1.0.

(3) Addition of the terrace level did not substantially affect the flow field downstream of the downwind building.

(4) The normalized longitudinal distance to reattachment behind the downwind building model increased with the building height, but the separation distance between the twin building models did not influence the reattachment

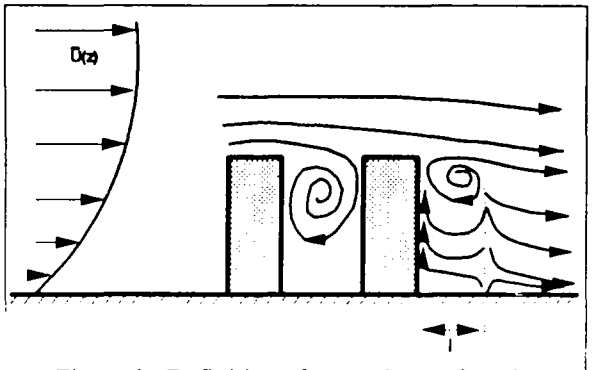

Figure 9. Definition of reattachment length.

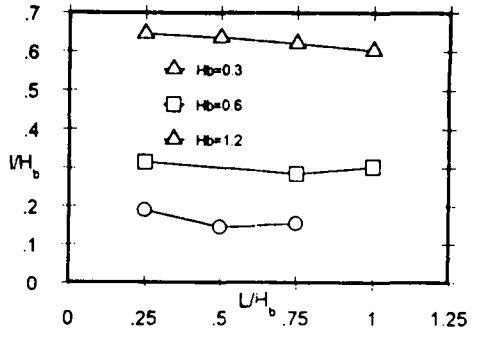

Figure 10. Reattachment length vs. building separation.

length for separation distances in the range of $0.25 \leq L/H_b \leq 1.0$.

(4) Mean flow streamlines show that location of emission sources near the downwind base of any of the buildings will lead to a potential for contaminating the downwind building face.

Efforts are underway to model both the flow field and dispersion characteristics using a k-ε numerical model. These data will provide comparative measurements against which the model will be compared and evaluated.

REFERENCES

Britter, R.E. & Hunt, J.C.R., 1979: Velocity Measurements and Order of Magnitude Estimates of the Flow Between Two Buildings in a Simulated Atmospheric Boundary Layer. *J. Indus. Aerodyn.*, 4, 165-82.

Cook, N.J., 1973: On Simulating the Lower Third of the Urban Adiabatic Boundary Layer in a Wind Tunnel. *Atmos. Envir.*, 7, 691-706.

Davies, M.E., Quincey, V.G. & Tindall, S.J., 1980: The Near-Wake of a Tall Building Block in Uniform and Turbulent Flows. Proc. 5th Int. Conf. Wind Engr., Fort Collins, CO, July, 1979 (J.E. Cermak, ed.), v. 1, p.289-98. Pergamon Press, NY, NY.

ESDU, 1972: Characteristics of Wind Speed in the Lower Layers of the Atmosphere near the Ground: Strong Winds (Neutral Atmosphere). Item No. 72026, Engineering Sciences Data Unit, London, UK.

Golden, J., 1961: Scale Model Techniques. M.S. Thesis, College of Engr.,New York Univ., NY, NY, 48p.

Irwin, H.P.A.H., 1981: The Design of Spires for Wind Simulation. *J. Wind Engr. Indus. Aerodyn.*, 7, 361-66.

Kaimal, J.C., Wyngaard, J.C., Izumi, Y. & Cote, O.R., 1972: Spectral Characteristics of Surface Layer Turbulence. *Quart. J. Roy. Meteorol. Soc.*, 98, 563-89.

Ohba, M. and Lawson, R.E., Jr., 1993: Physical Modeling of Concentration Distributions Around Twin High-Rise Buildings With a District Heating Plant. AMS Eighth Joint Conf. On Applications of Air Pollution Meteorology, Jan 23-28, Nashville, TN.

Snyder, W.H., 1981: Guideline for Fluid Modeling of Atmospheric Diffusion. Rpt. No. EPA-600/8-81-009,Envir. Prot. Agcy., Res. Tri. Pk., NC, 200p.

Wise, A.F.E., 1971: Effects Due to Groups of Buildings. *Phil. Trans. Roy. Soc. Lond.*, A, 469-85.

TECHNICAL REPORT DATA

(Please read Instructions on the reverse before completi

1. REPORT NO.	2.	3.
EPA/600/A-93/292		

4. TITLE AND SUBTITLE	5. REPORT DATE
Physical Modeling of the Flow Field Around Twin High-Rise Buildings	1993
	6. PERFORMING ORGANIZATION CODE
7. AUTHOR(S)	8. PERFORMING ORGANIZATION REPORT NO.
Robert E. Lawson, Jr.[1] and Masaaki Ohba[2]	
9. PERFORMING ORGANIZATION NAME AND ADDRESS	10. PROGRAM ELEMENT NO.
Atmospheric Research & Exposure Assessment Laboratory Office of Research and Development U.S. Environmental Protection Agency Research Triangle Park, North Carolina 27711	11. CONTRACT/GRANT NO.
12. SPONSORING AGENCY NAME AND ADDRESS	13. TYPE OF REPORT AND PERIOD COVERED
Atmospheric Research & Exposure Assessment Laboratory-RTP, NC Office of Research and Development U.S. Environmental Protection Agency Research Triangle Park, NC 27711	Presentation
	14. SPONSORING AGENCY CODE EPA/600/09

15. SUPPLEMENTARY NOTES

Presentation: AMS Eighth Joint Conf. on Applications of Air Pollution Meteor., Jan., 1994, Nashville, TN.

[1] On assignment from the National Oceanic and Atmos. Admin., US Dept. of Commerce

[2] Tokyo Institute of Polytechnics, Atsugi, Kanagawa Pref., Japan 243-02

16. ABSTRACT

A wind tunnel study was conducted to investigate the flow characteristics near three configurations of high-rise buildings - an isolated high-rise building, two high-rise buildings separated in the streamwise direction, and two high-rise buildings separated in the streamwise direction, but situated atop a terrace-shaped lower level. A pulsed-wire anemometer was used with an automated traversing system to make detailed velocity measurements in the vertical centerplane and in a horizontal plane just above the surface. For each of the three basic configurations, measurements were taken while systematically varying the building height or, for the twin buildings, varying both the height and separation between the buildings. The measured mean velocity components were used to construct plots showing velocity vectors and streamline patterns and, hence, the height and downwind extent of areas of recirculating flow. The mean flow streamline plots were used to identify emission source locations that might result in adverse concentrations on the downwind building face.

17. KEY WORDS AND DOCUMENT ANALYSIS

a. DESCRIPTORS	b. IDENTIFIERS/OPEN ENDED TERMS	c. COSATI Field/Group

18. DISTRIBUTION STATEMENT	19. SECURITY CLASS 27(This Report)	21. NO. OF PAGES
RELEASE TO PUBLIC	UNCLASSIFIED	8
	20. SECURITY CLASS 27(This page)	22. PRICE
	UNCLASSIFIED	